NANOSYSTEMS:
PHYSICS, CHEMISTRY, MATHEMATICS

Original article

Naqash A.N., Shah K.A., et al. *Nanosystems: Phys. Chem. Math.*, 2023, **14** (4), 438–446.
http://nanojournal.ifmo.ru
DOI 10.17586/2220-8054-2023-14-4-438-446

Transport properties of GaAs Co-doped H-passivated low-buckled and high-buckled zigzag silicene nanoribbon two probe devices

Asma N. Naqash[1,2], Khurshed A. Shah[1,3], Javid Ahmad Sheikh[2], Brijesh Kumbhani[4], Syed Muzaffar Ali Andrabi[5]

[1]Department of Nanotechnology, University of Kashmir, Srinagar, Jammu and Kashmir – 190006, India

[2]Department of Electronics and Instrumentation Technology, University of Kashmir, Srinagar, Jammu and Kashmir – 190006, India

[3]Postgraduate Department of Physics, S. P. College, Cluster University Srinagar, Jammu and Kashmir – 190001, India

[4]Department of Electrical Engineering, Indian Institute of Technology Ropar, Punjab – 140001, India

[5]Department of Applied Sciences, Institute of Technology, Zakura Campus, University of Kashmir, Srinagar, Jammu and Kashmir – 190006, India

Corresponding author: Khurshed A. Shah, drkhursheda@gmail.com

ABSTRACT In this study, we have investigated the transport properties of low bucked (LB) and high buckled (HB) silicene based two probe devices such as I–V characteristics, conductance, transmission spectrum and projected device density of states. Firstly, we have opened a bandgap in both LB and HB zigzag silicene nanoribbon (ZSiNR) by hydrogen passivation and simulated for their transport properties. Further, we have doped the LB and HB ZSiNR structures by gallium (Ga) and arsenide (As) atoms in order to determine their changes in the transport properties. The results show that 4 atom width silicene nanoribbon shows a maximum band gap of 2.76 and 2.72 Å for LB-ZSiNR and HB-ZSiNR, respectively. The 2 atom doped ZSiNR shows good transport characteristics in the voltage range of 0.5 to 1.5 V in comparison with 4 and 6 atom doped models. The obtained results were validated by calculating the transmission spectrum and projected device density of states. It is believed that the modelled devices will find number of futuristic applications in the electronic industry.

KEYWORDS zigzag silicene nanoribbons, DFT, I-V characteristics, transmission spectra, PDDoS

ACKNOWLEDGEMENTS This work was supported by JKST&IC funded project (Grant No. JKST&IC/SRE/1172-74).

FOR CITATION Naqash A.N., Shah K.A., Sheikh J., Kumbhani B., Andrabi S.M.A. Transport properties of GaAs Co-doped H-passivated low-buckled and high-buckled zigzag silicene nanoribbon two probe devices. *Nanosystems: Phys. Chem. Math.*, 2023, **14** (4), 438–446.

1. Introduction

The silicene, a honeycomb (hexagonal) structured 2D material exfoliated from silicon monolayer atoms, is exceptionally expedient over graphene due to its sp3 hybridization. Silicene does not exist in nature and tends to generate larger silicone crystals and silicone compounds [1]. The effective synthesis of this element on metal substrates [2–4] has spurred interest in both theoretical [5, 6] and experimental investigations [7, 8]. The buckled structure of 2D silicene result either from the weak π double bonds due to the parted Si atoms or through the pseudo-Jahn–Teller distortions (PJT) [9]. Due to the zero band gap semimetal character with linearly crossing bands at the Fermi level (EF), the charge carriers move like massless fermions at around 10^6 m/s at the Dirac point. This could be fixed by directing various modulation techniques for recognition of tunable band gaps. A number of such formulations include modeling silicene into nanoribbon (NR) bands of atomic layer width and chemical functionalization [10–13]. In addition, the implementation of strain, the application of an external electrical field [14], vacancy creation [15], surface adsorption, substitution, nano-mesh creation (creating nanoholes on the silicene sheet), etc. could also yield band gap efficiently [16]. There have been some reports proposed by Yao, et al. [17] showing the distinct properties of large spin–orbit coupling (SOC) effect as a result of buckling and the Quantum Spin Hall effect (QSHE) [18], and a valley-polarized metallic phase by Ezawa [19]. Due to such articulations in the silicene material, it finds several device implementations as field effect transistor (FET), tunnel field effect transistor (TFET), spintronics, valleytronics, bandgap engineering, gas sensors etc [16].

The atomic structure of silicene could be perceived into three phases based on the buckling done. The Planar structure (PL) (pristine version), as per the binding energy computations of silicene, has a greater energy than its Low-buckled (LB) and High-buckled (HB) complements. There exist fictitious phonon frequencies in the PL structure for the majority of the Brillouin zone [20] that renders it unstable. The fictitious phonon frequencies are moreover evident in silicene HB structures with significant buckling heights of 2 Å. As a result, HB structures are not consistent to actual local minima over the Born–Oppenheimer surface [21]. Silicene's LB structures, on the other hand, exhibit phonon dispersion curves with positive coefficients over the whole Brillouin zone, making them dynamically stable [21].

Though the lack of a band gap restricts the material for both electronic and device applications, but optimistically functionalization, strain, or the application of an external electrical field, nano-mesh creation, defect creation, etc. can be implemented to yield a band gap. Another way of solving band gap problem is by slicing silicene into silicene nanoribbons (SiNRs). SiNRs are of two forms viz., Armchair Silicene Nanoribbons (ASiNRs) and Zigzag Silicene Nanoribbons (ZSiNRs) [3]. In the past, several elements like Al, Ga, In, Th, P, As, Sb and Bi have been investigated for various electronic (band structure, density of states (DOS)) and transport properties (transmission spectra and I–V characteristics) of silicene NRs [20]. Likewise, dopants containing Gallium and Arsenic have been implemented for the semiconductor simulation [22, 23].

Gallium belongs to group-III with valency three and arsenic belongs to group-V with valency five in the periodic table. Thus, Gallium atoms are often replaced for doping in p-type semiconductors with majority of the charge carriers as holes and contrast to this arsenic atoms are replaced to dope in n-type semiconductors. Ga and As are mostly used for optoelectronic applications because of their optical properties [24, 25]. Further, the lattice constants of Ga and As are identical [3]. Gallium arsenide is formed by coupling Group III and V elements for implementation as photo detectors, LEDs etc. [26].

The ZSiNRs have been used for various applications such as giant magnetoresistance [27], high hydrogen storage capacity [28], lithium storage [29], spin-filtering [30, 31], magnetic random access memory and digital logic [32], spin polarization [33], etc. In this study, for the first time, we have studied the transport characteristics of GaAs co-doped hydrogen passivated low-buckled (LB) and high-buckled (HB) ZSiNR at various GaAs doping levels. The device is distinctly doped with 2, 4 and 6 GaAs atoms and their transport characteristics are investigated. The studies revealed that doped LB and HB ZSiNR devices have distinct I-V and conductance curves, transmission spectra and device density of states.

2. Models and methods

The current study has been carried out utilizing the density functional theory (DFT) and non-equilibrium Green's Function (NEGF) operations [2], based on the software Atomistic Tool Kit (ATK) software version P-2019.03 and its graphical user interface Virtual Nanolab (VNL) [34]. We project a two-probe device with three zones, the left electrode, the middle scattering region, and the right electrode in order to compute the transport properties. The device is represented in Fig. 1. Electrodes are assimilated into the ZSiNR structure to eliminate the current quantization effects induced by contact regions. The Silicon–Silicon bond length is set at 2.28 Å. The buckling height for the low buckled and the high buckled structures are taken as 0.44 and 0.54 Å, respectively.

Electron density expansion is treated with double zeta polarised basis set that interprets the electron wave function. Also density mesh cut-off is set at 75 Hartee (150 Ry). With a 15 Å vacuum separation along the zigzag silicene nanoribbons (ZSiNR)'s width, the interlayer interactions are circumvented. The Local Density Approximation (LDA) is used to account for the exchange-correlation interactions, which is a basic approximation, whereas Generalized Gradient Approximation (GGA) is an advanced version of LDA and the LDA approximation has been used for the band structure calculations in various structures [2, 38, 39]. The atomic locations and asymmetric lattice constants are relaxed up to a maximum force of 0.01 eV. For sampling during the structure optimization, the Brillouin zone has been sampled at $1 \times 1 \times 21$ k-points and for the computation of band structure, device density of states and electron transport calculations, a $1 \times 1 \times 125$ Monkhorst-Pack K-points grid is selected along the ZSiNR growth direction (z-direction). The "limited-memory Broyden–Fletcher–Goldfarb–Shanno" (LBFGS) algorithm has been employed for structure optimization [35]. The electrode temperature of the models has been set to 300K for operation. The current across the electrodes is analyzed by voltage bias of 0 to 2 V. Table 1 below depicts the simulation parameters implemented in the modulation of the two probe device.

3. Results and discussions

In order to investigate silicene for device applications, it is important to open the bandgap in the material. In this study, we have H-passivated the ZSiNR and varied its width to investigate the change in band gap in the material as shown in Fig. 2. From the curves, it is clear that for both LB and HB ZSiNR the increase in the width of the nanoribbon results in the decrease of the energy gap which is in agreement with the literature [16, 36] and the 4 atom width LB–H–ZSiNR and HB–H–ZSiNR shows a maximum band gap of 2.76 and 2.72 Å, respectively.

Silicene is a two-dimensional material composed of a single layer of silicon atoms arranged in a honeycomb lattice, similar to graphene. Its atomic structure could be perceived into three phases based on the buckling done. The Planar

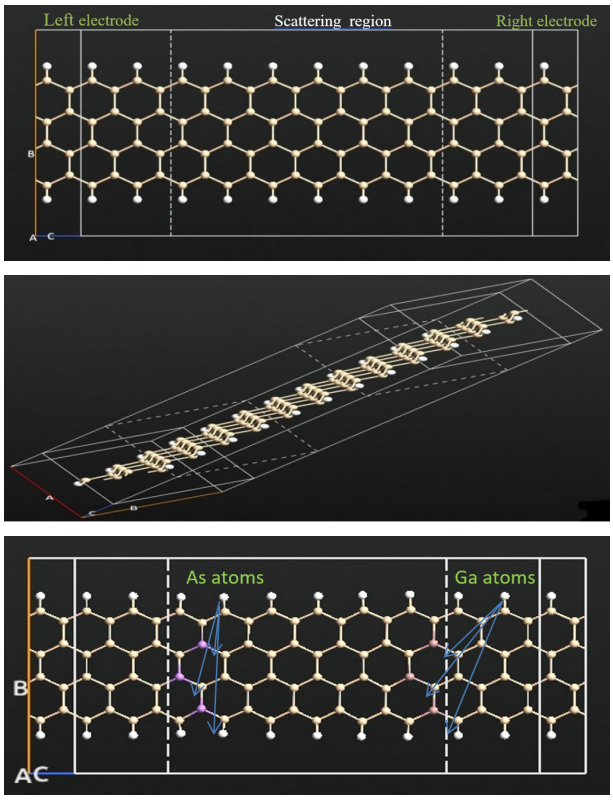

FIG. 1. H-passivated zigzag silicene nanoribbon (ZSiNR) two probe modeled device: (a) – top-view; (b) – side-view; (c) – GaAs co-doped

TABLE 1. The simulation parameters implemented in the modeled two probe devices

Parameter	**Value**
Calculator	Linear Combination of Atomic Orbitals (LCAO)
Formalism	DFT
Pseudopotential	FHI (Martins–Troullier Type)
Exchange-correlation functional	LDA
Density mesh cut-off Energy	75 Hartee
k-point sampling	1, 1, 125
Basis set	Double-ζ polarization (DZP)
Electrode Temperature	300 K
Device Algorithm Formalism	Non-equilibrium Green's Function (NEGF)
Poisson Solver	FFT2D

structure (PL) (pristine version), as per the binding energy computations of silicene, has a greater energy than its Low-buckled (LB) and High-buckled (HB) complements. In planar silicene there is no bandgap while the high buckled silicene with buckling height of 2 Å is unstable [16]. The rise in buckling height suggests that silicene's atomic orbitals have a higher concentration of the more stable sp3 hybridization than sp2 hybridization. We have inspected two stable buckling heights of 0.44 and 0.54 Å in the middle range of the low buckled silicene, as illustrated in Fig. 2. Consequently, we have labeled them as Low buckle (LB) for 0.44 Å and High buckled (HB) for 0.54 Å, respectively.

In the low buckled (i.e., 0.44 Å) silicene nanoribbon, the silicon atoms are arranged in a planar configuration with minimal vertical displacement (buckling) from the plane of the nanoribbon. This arrangement leads to a relatively large inter-atomic spacing and weaker silicon-silicon bonds. The weak bonding results in a smaller bandgap since the energy required to promote electrons from the valence band to the conduction band is lower. As the width of the low buckled

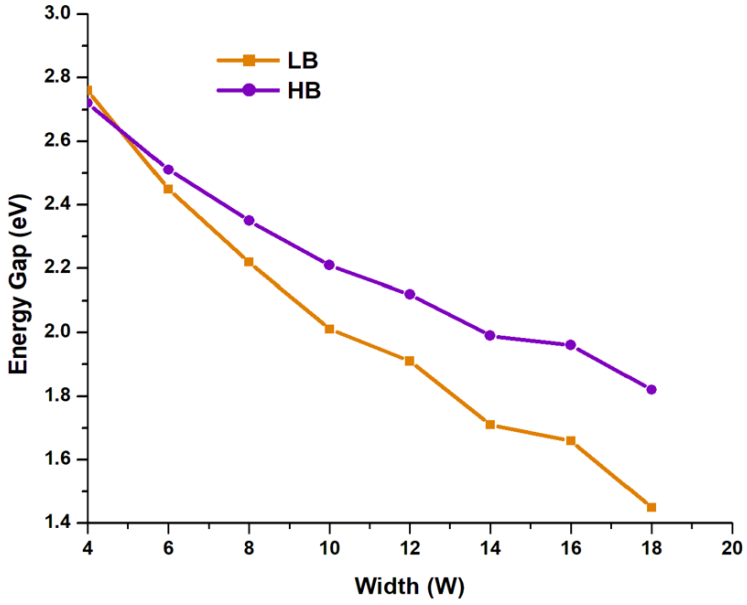

FIG. 2. Variation of bandgap of H-passivated low-buckled (LB) and high-buckled (HB) ZSiNRs with the change in width of the silicene nanoribbon

nanoribbon decreases, the distance between silicon atoms decreases, resulting in strengthening of bonds, and consequently increasing the bandgap. In other words, as the width increases the band gap decreases.

On the other hand, in the high buckled (0.54 Å) silicene nanoribbon, the silicon atoms exhibit a more pronounced vertical displacement or buckling from the nanoribbon plane. This buckling causes the atoms to be closer together, leading to stronger silicon-silicon bonds. The stronger bonding results in a larger bandgap since more energy is required to promote electrons across the wider bandgap (wider than the low LB counterpart). As the width of the high buckled nanoribbon decreases, the interatomic spacing remains relatively constant due to the buckling pattern, which keeps the bandgap more stable or possibly even increasing slightly. It's important to note that the exact behavior of the bandgap with respect to decreasing width may also be influenced by the nanoribbon's specific edge configuration, strain effects, and other environmental factors and the quantum confinement effects can play a role in modifying the electronic properties of narrow nanoribbons [16]. Therefore, detailed theoretical calculations or simulations may be necessary to precisely predict the bandgap changes in low and high buckled silicene nanoribbons as their width varies.

The transport characteristics and the impact of various doping levels on the current and conductance of the ZSiNR two-probe systems have been explored. The remaining forces on each atom were reduced to less than 0.05 eV/A by relaxing each of the structures completely. We have obtained the I–V curves, conductance curves, transmission spectra and projected device density of states (PDDoS) of the LB–ZSiNR and HB–ZSiNR modeled devices. These curves (Figs. 4–6) depict the transport mechanism of the models in the similar manner as does the IV curves [40–43].

The variation in I–V curves of low-buckled and high-buckled ZSiNR modeled devices with different doping levels are shown in Fig. 3(a) and Fig. 3(b) respectively.

From Fig. 3(a) and Fig. 3(b), it is clear that the 2 atoms doped GaAs LB and HB ZSiNR modeled device conducts more as compared to 4 atoms doped GaAs LB and HB ZSiNR devices and the change is significant in the bias range of 0.5 to 1.5 V. However, in LB and HB pristine ZSiNR devices the increase in current is significant in 1.5 to 2 V voltage range which is in agreement with the result reported in the literature [30]. The conductance curves of the modeled devices are depicted in Fig. 4(a) and Fig. 4(b). The conductance of the 2 atoms doped GaAs LB–ZSiNR and HB–ZSiNR modeled devices is higher than the corresponding 4 atoms doped structures particularly in the bias window of 0.5 to 1.5 V which is in agreement with the above observed I–V characteristics.

We further inspected the transmission spectra of the modeled structures to better comprehend the I–V curves at 0.2 V. Fig. 5 and Fig. 6 show the transmission spectra of LB and HB ZSiNR for different doping concentrations. The probability of the occupancy of the states is represented by black, red and green lines for pristine, 2 atoms doped, 4 atoms doped ZSiNRs, respectively. It can be observed from Fig. 5 and Fig. 6 that the transmission peaks with reference to the pristine model are larger than the corresponding peaks of doped models at the applied voltage of 0.2 V. Thus supporting the statement for reduced current in the doped models as compared to the pristine silicene devices. Furthermore, from Fig. 5 and Fig. 6, it is clear that the 2 atoms doped model shows better transmission peaks as compared to the highly doped models. In addition, the transmission is good in the bias range of 0.5 to 1.5 V that is also in agreement with the obtained I–V and conductance curves (refer Fig. 3 and Fig. 4).

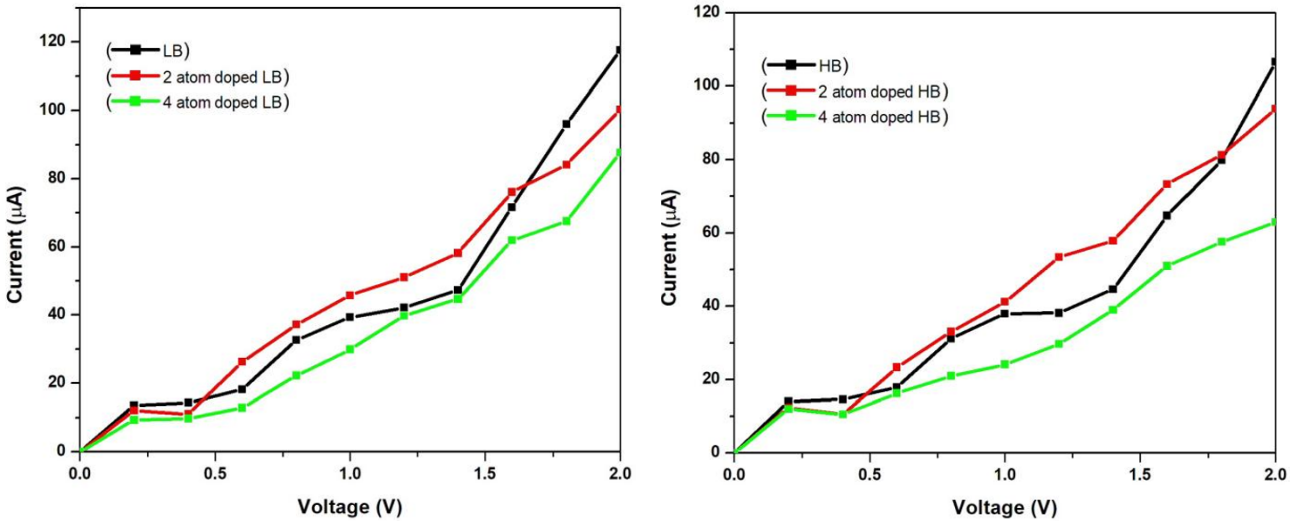

(a) (b)

FIG. 3. I–V curves of H-passivated (a) low-buckled (LB) ZSiNR (b) high-buckled (HB) ZSiNR two probe devices

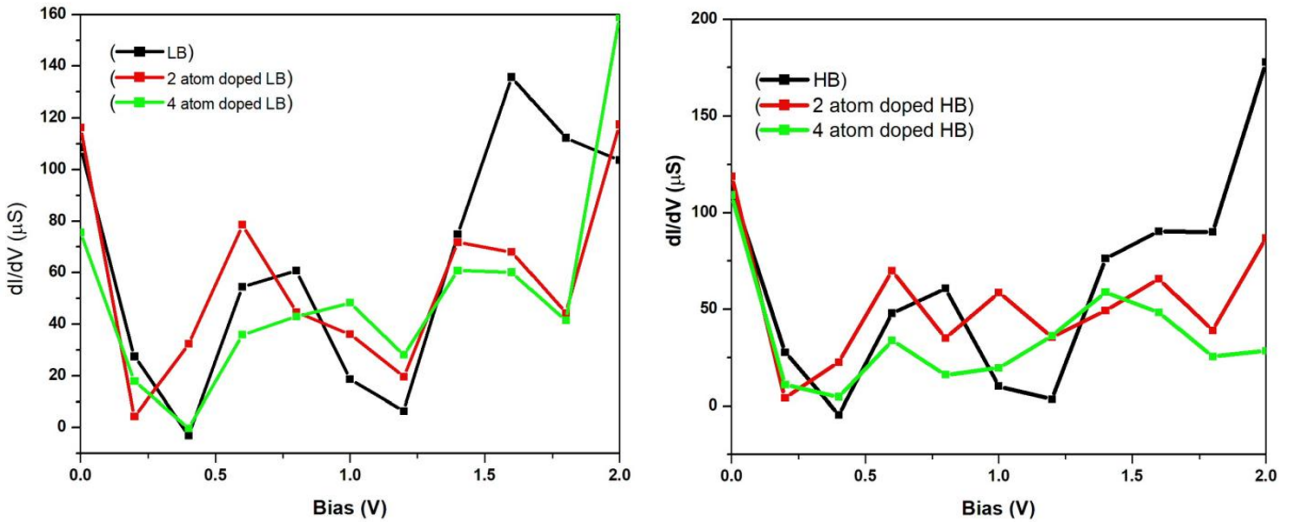

(a) (b)

FIG. 4. Conductance curves of H-passivated (a) LB–ZSiNR (b) HB–ZSiNR two probe devices

The PDDoS numerically depicts the density distribution of states. The PDDoS specifies the number of states the quantum carriers are permitted to occupy at a specific energy level.

The ATK software implements the spectral density matrix tool for its computation:

$$\rho\left(E\right) = \rho^{L}\left(E\right) + \rho^{R}\left(E\right). \tag{1}$$

Here, L and R stand for the corresponding contributions of the left and right electrodes.

The relation for local density of states (LDoS) is given by

$$D\left(E,\ r\right) = \sum_{ij} \rho_{ij}\left(E\right) \emptyset_i(r)\emptyset_j(r), \tag{2}$$

where the basis set orbitals $\emptyset_i(r)$ are real functions in ATK obtained by using the solid harmonics.

Integrating the LDoS over the whole space, PDDoS can be computed as follows;

$$D\left(E\right) = \int drD\left(E,r\right) = \sum_{ij} \rho_{ij}\left(E\right) S_{ij}, \tag{3}$$

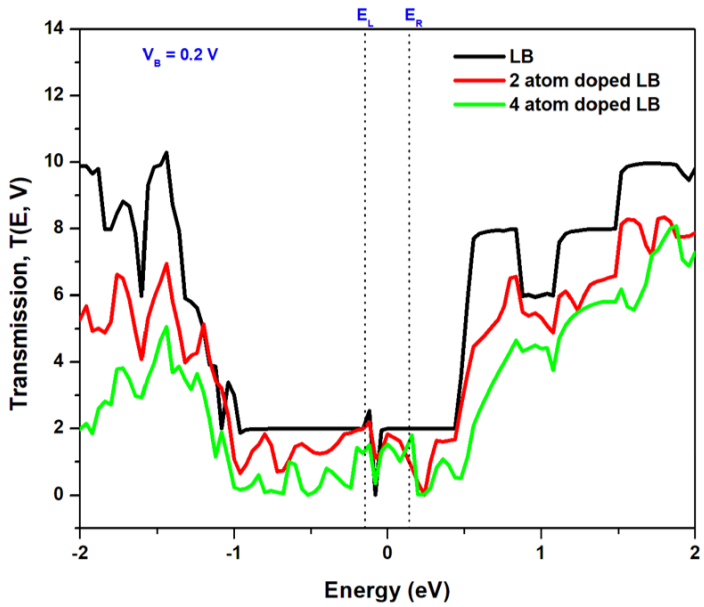

FIG. 5. Transmission spectra of H-passivated LB–ZSiNR for different doping concentrations

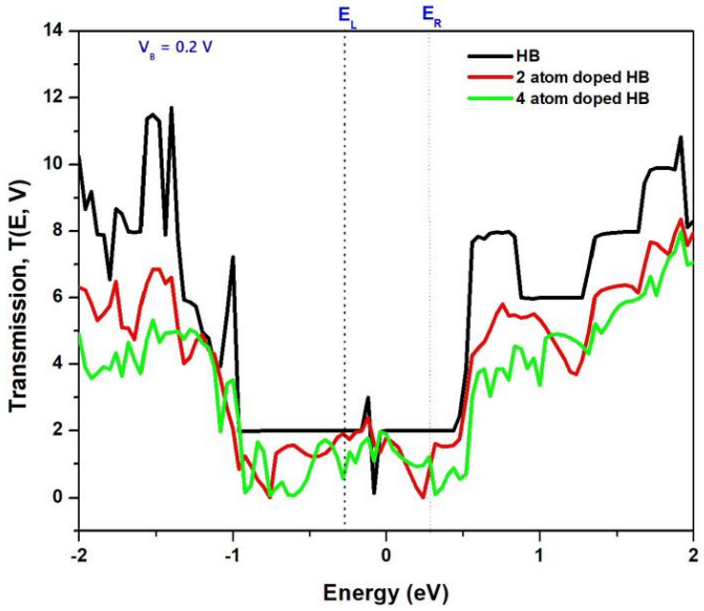

FIG. 6. Transmission spectra of H-passivated HB–ZSiNR for different doping concentrations

where $S_{ij} = \int \emptyset_i(r)\,\emptyset_j(r)\,dr$ is the overlap matrix.

The PDDoS of LB and HB H-passivated ZSiNR at different doping levels is shown in Fig. 7. From Fig. 7, it is clear that very small peaks occur below the Fermi level in the pristine and doped ZSiNRs which means that a fewer number of available energy states are presented in the valence band. Furthermore, peaks are also observed above the Fermi level in the conduction band of the both the pristine and the doped ZSiNR models. Thus, the results depict that conductivity is possible for the proposed devices as the occupancy level is sufficient at both the valence and the conduction bands [37].

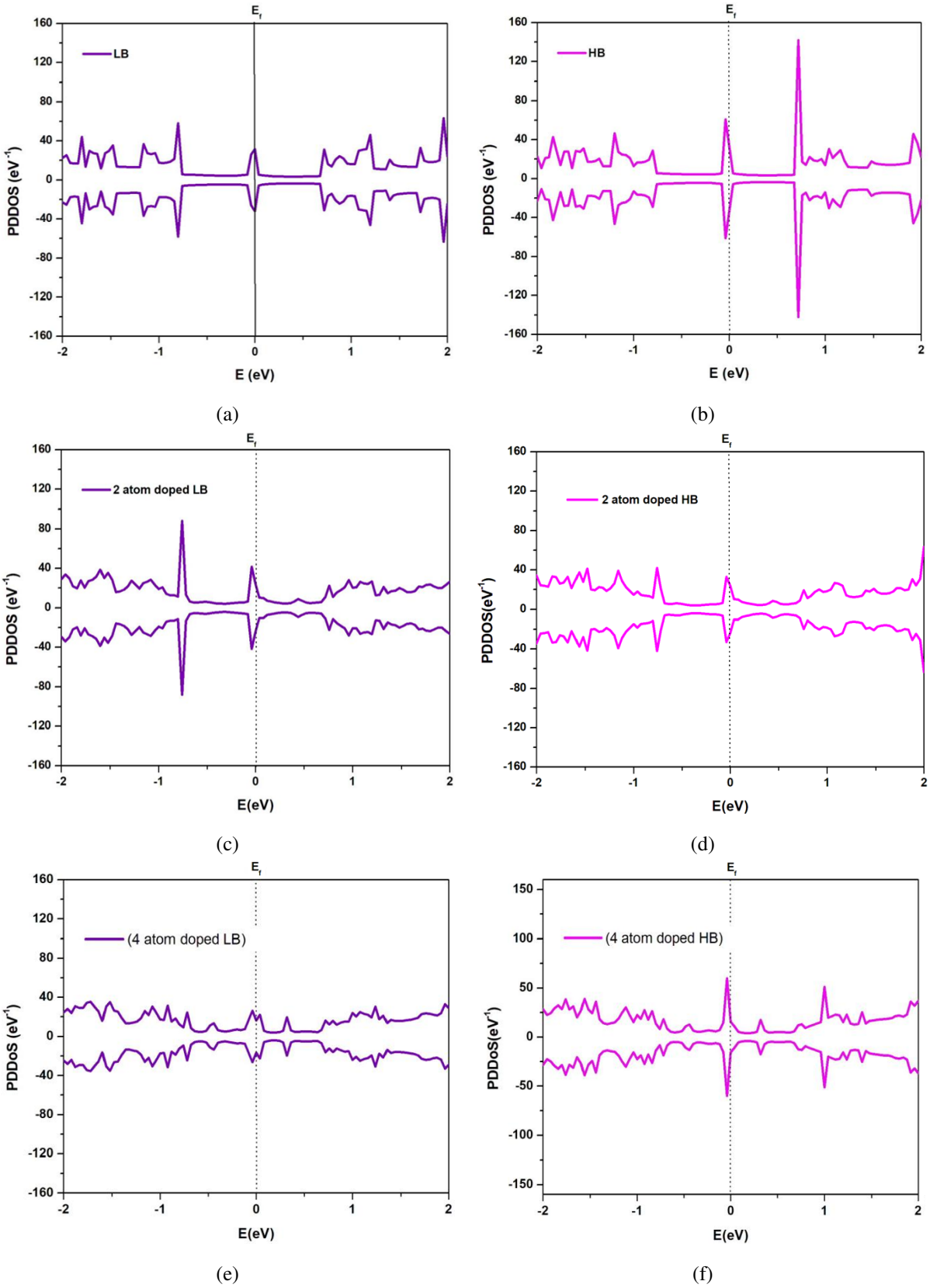

FIG. 7. PDDoS at different doping levels of LB and HB (a) pristine LB, (b) pristine HB, (c) 2 atom doped LB, (d) 2 atom doped HB, (e) 4 atom doped LB, and (f) 4 atom doped HBH-passivated ZSiNR

4. Conclusions

In this study, we have modelled and simulated both pristine and doped low buckled (LB) and high buckled (LB) ZSiNR two probe devices using DFT in combination with NEGF formalism and calculated their I–V characteristics, conductance, transmission spectrum and project device density of states (PDDoS). The results show that the level of buckling in the silicene structures changes the characteristics of the devices which are further dependent on the magnitude of the applied voltage. The doping by gallium and arsenide atoms shows a profound effect on the I–V characteristics and conductance of modelled two probe devices, particularly, in the middle applied voltage range and it is sensitive to the level of doping. The low level doping shows higher magnitude of current than the high level doping. Furthermore, the transmission spectrum and PDDoS completely agree with the I–V and conductance curves. The results are important from both basic and applied points of view.

References

[1] Motamedi M. A space structural mechanics model of silicene. *Proceedings of the Institution of Mechanical Engineers, Part N: J. of Nanomaterials, Nanoengineering and Nanosystems*, 2020, **234** (1–2), P. 3–10.

[2] Zhao J., Liu H., Yu Z., Quhe R., Zhou S., Wang Y., Liu C.C., et al. Rise of silicene: A competitive 2D material. *Progress in Materials Science*, 2016, **83**, P. 24–151.

[3] Aufray B., Kara A., Vizzini S., Oughaddou H., Léandri C., Ealet B., Lay G.L. Graphene-like silicon nanoribbons on Ag (110): A possible formation of silicene. *Applied Physics Letters*, 2010, **96** (18), 183102.

[4] Padova P.D., Quaresima C., Ottaviani C., Sheverdyaeva P.M., Moras P., Carbone C., Topwal D., et al. Evidence of graphene-like electronic signature in silicene nanoribbons. *Applied Physics Letters*, 2010, **96** (26), 261905.

[5] Lalmi B., Oughaddou H., Enriquez H., Kara A., Vizzini S., Ealet B., Aufray B. Epitaxial growth of a silicene sheet. *Applied Physics Letters*, 2010, **97** (22), 223109.

[6] Fagan S.B., Baierle R.J., Mota R., da Silva A.J.R., Fazzio A. Ab initio calculations for a hypothetical material: Silicon nanotubes. *Physical Review B*, 2000, **61** (15), 9994.

[7] Cahangirov S., Topsakal M., Aktürk E., Şahin H., Ciraci S. Two- and one-dimensional honeycomb structures of silicon and germanium. *Physical Review Letters*, 2009, **102** (23), 236804.

[8] Chen Lan, Liu C.C., Feng B., He X., Cheng P., Ding Z., Meng S., Yao Y., Wu K. Evidence for Dirac fermions in a honeycomb lattice based on silicon. *Physical Review Letters*, 2012, **109** (5), 056804.

[9] Guzmán-Verri G.G., Lew Yan Voon L.C. Electronic structure of silicon-based nanostructures. *Physical Review B*, 2007, **76** (7), 075131.

[10] Deepthi Jose, Ayan Datta. Understanding of the buckling distortions in silicene. *J. of Physical Chemistry C*, 2012, **116** (46), P. 24639–24648.

[11] Ding Yi, Jun Ni. Electronic structures of silicon nanoribbons. *Applied Physics Letters*, 2009, **95** (8), 083115.

[12] Ding Yi, Yanli Wang. Density functional theory study of the silicene-like SiX and XSi_3 (X= B, C, N, Al, P) honeycomb lattices: the various buckled structures and versatile electronic properties. *J. of Physical Chemistry C*, 2013, **117** (35), P. 18266–18278.

[13] Ni Zeyuan, Qihang Liu, Kechao Tang, Jiaxin Zheng, Jing Zhou, Rui Qin, Zhengxiang Gao, Dapeng Yu, Jing Lu. Tunable bandgap in silicene and germanene. *Nano Letters*, 2012, **12** (1), P. 113–118.

[14] Sahin H., Cahangirov S., Topsakal M., Bekaroglu E., Akturk E., Senger R.T., Ciraci S. Monolayer honeycomb structures of group-IV elements and III-V binary compounds: First-principles calculations. *Physical Review B*, 2009, **80** (15), 155453.

[15] Iordanidou K., Houssa M., van den Broek B., Pourtois G., Afanas'ev V.V., Stesmans A. Impact of point defects on the electronic and transport properties of silicenenanoribbons. *J. of Physics: Condensed Matter*, 2016, **28** (3), 035302.

[16] Kharadi M.A., Malik G.F.A., Khanday F.A., Shah K.A., Mittal S., Kaushik B.K. Review – Silicene: From material to device applications. *ECS J. of Solid State Science and Technology*, 2020, **9** (11), 115031.

[17] Liu C.C., Hua Jiang, Yugui Yao. Low-energy effective Hamiltonian involving spin-orbit coupling in silicene and two-dimensional germanium and tin. *Physical Review B*, 2011, **84** (19), 195430.

[18] Liu C.C., Wanxiang Feng, Yugui Yao. Quantum spin Hall effect in silicene and two-dimensional germanium. *Physical Review Letters*, 2011, **107** (7), 076802.

[19] Motohiko E. Valley-polarized metals and quantum anomalous Hall effect in silicene. *Physical Review Letters*, 2012, **109** (5), 055502.

[20] Das R., Chowdhury S., Majumdar A., Jana D. Optical properties of P and Al doped silicene: a first principles study. *RSC Advances*, 2015, **5** (1), P. 41–50.

[21] Saleh Bahaa E.A., Malvin Carl Teich. *Fundamentals of Photonics*. John Wiley & Sons. Inc., Hoboken N.J., 1991.

[22] Chen Xuanhu, Fangfang Ren, Shulin Gu, Jiandong Ye. Review of gallium-oxide-based solar-blind ultraviolet photodetectors. *Photonics Research*, 2019, **7** (4), P. 381–415.

[23] Edelman P. Environmental and workplace contamination in the semiconductor industry: implications for future health of the workforce and community. *Environmental Health Perspectives*, 1990, **86**, P. 291–295.

[24] Shinde S.S., Shinde P.S., Oh Y.W., Haranath D., Bhosale C.H., Rajpure K.Y. Structural, optoelectronic, luminescence and thermal properties of Ga-doped zinc oxide thin films. *Applied Surface Science*, 2012, **258** (24), P. 9969–9976.

[25] Brodsky M.H. Progress in gallium arsenide semiconductors. *Scientific American*, 1990, **262** (2), P. 68–75.

[26] Ding He, Hao Hong, Dali Cheng, Zhao Shi, Kaihui Liu, Xing Sheng. Power-and spectral-dependent photon-recycling effects in a double-junction gallium arsenide photodiode. *ACS Photonics*, 2019, **6** (1), P. 59–65.

[27] Xu Chengyong, Guangfu Luo, Qihang Liu, Jiaxin Zheng, Zhimeng Zhang, Shigeru Nagase, Zhengxiang Gao, Jing Lu. Giant magnetoresistance in silicene nanoribbons. *Nanoscale*, 2012, **4** (10), P. 3111–3117.

[28] Li Feng, Changwen Zhang, Wei-Xiao Ji, Mingwen Zhao. High hydrogen storage capacity in calcium-decorated silicene nanostructures. *Physica Status Solidi B*, 2015, **252** (9), P. 2072–2078.

[29] Guo Gang, Yuliang Mao, Jianxin Zhong, Jianmei Yuan, Hongquan Zhao. Design lithium storage materials by lithium adatoms adsorption at the edges of zigzag silicenenanoribbon: a first principle study. *Applied Surface Science*, 2017, **406**, P. 161–169.

[30] Kharadi M.A., Malik G.F.A., Khanday F.A., Shah K.A. Hydrogenated silicene based magnetic junction with improved tunneling magnetoresistance and spin-filtering efficiency. *Physics Letters A*, 2020, **384** (32), 126826.

[31] Kharadi M.A., Malik G.F.A., Khanday F.A., Mittal S. Silicene-based spin filter with high spin-polarization. *IEEE Transactions on Electron Devices*, 2021, **68** (10), P. 5095–5100.

[32] Gani Muzafar, Khurshed Ahmad Shah, Shabir A. Parah. Realization of a sub 10-nm silicene magnetic tunnel junction and its application for magnetic random access memory and digital logic. *IEEE Transactions on Nanotechnology*, 2021, **20**, P. 466–473.
[33] Kharadi M.A., Malik G.F.A., Mittal S. Electric field tunable spin polarization in functionalized silicene. *Physics Letters A*, 2022, **429**, 127952.
[34] Quantum ATK version P-2019.03, synopsis quantum ATK. URL: https://www.synopsys.com/silicon/quantumatk.html.
[35] Saputro Dewi Retno Sari, Purnami Widyaningsih. Limited memory Broyden-Fletcher-Goldfarb-Shanno (L-BFGS) method for the parameter estimation on geographically weighted ordinal logistic regression model (GWOLR). *AIP Conference Proceedings*, 2017, **1868** (1), 040009.
[36] Ding Yi, Jun Ni. Electronic structures of silicon nanoribbons. *Applied Physics Letters*, 2009, **95** (8), 083115.
[37] Parvaiz Shunaid M., Shah K.A., Dar G.N., Farooq Ahmad Khanday. Electrical doping in single walled carbon nanotube systems: A new technique. *Computational Condensed Matter*, 2020, **25**, e00507.
[38] Drummond N.D., Zolyomi V., Fal'ko V.I. Electrically tunable band gap in silicene. *Physical Review B*, 2012, **85** (7), 075423.
[39] Nigam S., Gupta S.K., Majumder C., Pandey R. Modulation of band gap by an applied electric field in silicene-based hetero-bilayers. *Physical Chemistry Chemical Physics*, 2015, **17**, P. 11324–11328.
[40] Jun K., Wu F., Li J. Symmetry-dependent transport properties and magnetoresistance in zigzag silicene nanoribbons. *Applied Physics Letters*, 2012, **100**, 233122.
[41] Kaur H., Kaur J., Kumar R. A Comparative Study on Electronic Transport Behavior of Silicene and B40-Nano Onions. *Silicon*, 2022, **14** (15), P. 9479–9487.
[42] Krishna S.M., Singh S., Kaushik B.K. Edge Modified Stanene Nanoribbons for Potential Nanointerconnects. *IEEE Transactions on Nanotechnology*, 2022, **22**, P. 1–8.
[43] Showket S., Shah K.A., Dar G.N. Pristine and Modified Silicene based Volatile Organic Compound Toxic Gas Sensor: A First Principles Study. *Physica Scripta*, 2023, **98**, 085937.

Submitted 12 June 2023; revised 18 August 2023; accepted 19 August 2023

Information about the authors:

Asma N. Naqash – Department of Nanotechnology and Department of Electronics and Instrumentation Technology, University of Kashmir, Srinagar, Jammu and Kashmir – 190006, India; asma.naqash@gmail.com

Khurshed A. Shah – Department of Nanotechnology, University of Kashmir, Srinagar, Jammu and Kashmir – 190006, India; Postgraduate Department of Physics, S. P. College, Cluster University Srinagar, Jammu and Kashmir – 190001, India; ORCID 0000-0002-2694-4515; drkhursheda@gmail.com

Javid Ahmad Sheikh – Department of Electronics and Instrumentation Technology, University of Kashmir, Srinagar, Jammu and Kashmir – 190006, India; ORCID 0000-0003-3113-3802; sheikhjavaid@uok.edu.in

Brijesh Kumbhani – Department of Electrical Engineering, Indian Institute of Technology Ropar, Punjab – 140001, India; brijesh@iitrpr.ac.in

Syed Muzaffar Ali Andrabi – Department of Applied Sciences, Institute of Technology, Zakura Campus, University of Kashmir, Srinagar, Jammu and Kashmir – 190006, India; muzaffar2000@gmail.com

Conflict of interest: the authors declare no conflict of interest.